Insect Biochemistry and Molecular Biology 110 (2019) 128–135

Contents lists available at ScienceDirect

Insect Biochemistry and Molecular Biology

journal homepage: www.elsevier.com/locate/ibmb

The putative chitin deacetylases Serpentine and Vermiform have non-redundant functions during *Drosophila* wing development

Min Zhang[a,1], Yanan Ji[a,1], Xubo Zhang[a,1], Pengjuan Ma[a], Yiwen Wang[b], Bernard Moussian[c,**], Jianzhen Zhang[a,*]

[a] Research Institute of Applied Biology, Shanxi University, Taiyuan, Shanxi, 030006, China
[b] Interfaculty Institute of Cell Biology, University of Tübingen, 72076 Tübingen, Germany
[c] Université Côte d'Azur, CNRS, Inserm, iBV, ParcValrose, 06108, Nice CEDEX 2, France

A B S T R A C T

The chitin modifying deacetylases (CDA) CDA1 and CDA2 have been reported to play partially redundant roles during insect cuticle formation and molting and tracheal morphogenesis in various insect species. In order to distinguish possible functional differences between these two enzymes, we analyzed their function during wing development in the fruit fly *Drosophila melanogaster*. In tissue-specific RNA interference experiments, we demonstrate that DmCDA1 (Serpentine, Serp) and DmCDA2 (Vermiform, Verm) have distinct functions during *Drosophila* adult wing cuticle differentiation. Chitosan staining revealed that Serp is the major enzyme responsible for chitin deacetylation during wing cuticle formation, while Verm does not seem to be needed for this process. Indeed, it is questionable whether Verm is a chitin deacetylase at all. Atomic force microscopy suggested that Serp and Verm have distinct roles in establishing the shape of nanoscale bumps at the wing surface. Moreover, our data indicate that Verm but not Serp is required for the laminar arrangement of chitin. Both enzymes participate in the establishment of the cuticular inward barrier against penetration of xenobiotics. Taken together, correct differentiation of the wing cuticle involves both Serp and Verm in parallel in largely non-overlapping functions.

1. Introduction

In order to adapt to external challenges, insects possess a cuticle that covers the whole body including appendages such as wings. The cuticle is composed of the polysaccharide chitin, proteins and lipids that are distributed in three major layers: the envelope, the epicuticle and the procuticle (Moussian, 2010). Chitin, the linear polymer of β-(1,4)-linked D-glucosamine, interacts with chitin-binding proteins forming a higher-order crystalline structure and thereby plays a critical role in shaping tissues of various forms, sizes and mechanical properties (Vincent and Wegst, 2004). Chitin deacetylases (CDA, EC 3.5.1.41), a member of extracellular chitin-modifying enzymes, are secreted metal-proteins that deacetylate chitin to partially convert chitin to chitosan (Tsigos et al., 2000). CDAs have been identified in fungi, nematodes, insects and other arthropods (Heustis et al., 2012; Vollmer and Tomasz, 2000; Xi et al., 2014). In insects, CDAs have been classified into five groups (group I–V) based on the presence of additional motifs (Dixit et al., 2008). Group I CDAs (CDA1 and CDA2) are the most studied enzymes, which have a CDA-like catalytic domain, a chitin-binding peritrophin-A domain (ChBD) in addition to a low-density lipoprotein receptor class A domain. Group I CDAs are required for the development of the tracheae and the cuticle (Arakane et al., 2009; Luschnig et al., 2006; Wang et al., 2006).

In previous works, it was repeatedly shown that group I CDAs in some insects have redundant functions. In *Drosophila melanogaster*, for instance, both Serpentine (Serp, DmCDA1) and Vermiform (Verm, DmCDA2) are required redundantly for chitin organisation in the cuticle and the tracheal system where they modify the structure of the luminal chitin matrix for controlled tracheal tube elongation (Luschnig et al., 2006; Wang et al., 2006). Interestingly, Dong et al. found that Serp, which was expressed in the fat body, was taken up by the tracheal cells and transmitted to the lumen to regulate tube length. By contrast, Verm played a key role on limiting tube length by a different mechanism (Dong et al., 2014). In the brown planthopper *Nilaparvata lugens*, injection of double-stranded RNAs against *NlCDA1* and *NlCDA2* caused lethality with similar phenotypes such as growth reduction and molting failure (Xi et al., 2014). Likewise, RNA interference (RNAi) against *Tribolium castaneum* group I *CDAs*, *TcCDA1* and *TcCDA2*, resulted in molting defects at different developmental stages and lethality (Arakane et al., 2009; Dixit et al., 2008). Recently, the same group reported that *TcCDA1* and *TcCDA2* were both required for the formation of higher structure chitin bundles in the *T. castaneum* cuticle (Noh

* Corresponding author.
** Corresponding author.
E-mail addresses: bernard.moussian@unice.fr (B. Moussian), zjz@sxu.edu.cn (J. Zhang).
[1] These authors contributed equally to this work.

https://doi.org/10.1016/j.ibmb.2019.05.008
Received 16 September 2018; Received in revised form 14 May 2019; Accepted 16 May 2019
Available online 18 May 2019
0965-1748/

et al., 2018).

In our laboratory, we found that in the migratory locust *Locusta migratoria* LmCDA1 and LmCDA2 located in an overlapping region of the cuticle and the functional differences between these two genes were observed based on RNAi combined with microscopic and ultrastructural observations (Yu et al., 2016, 2018). We reported that LmCDA1 regulated the thickness of chitin laminae through controlling chitin amounts and chitin deacetylation degree, whereas LmCDA2 controlled formation of the chitin laminae.

To explore the functional relationship between CDA1 and CDA2 in detail, we studied their function in wing cuticle formation in *D. melanogaster* by using a RNA interference (RNAi) approach. The use of the wing cuticle combines several advantages. Application of the Gal4/UAS expression system to generate wings with reduced *serp* or *verm* expression is not lethal allowing analyses of visible phenotypes in a comparably simple and large cuticular tissue. Indeed, the *D. melanogaster* pupal or adult wings can be conveniently dissected, manipulated and observed by microscopy. In this study, we combined the Gal4/UAS expression system with the Gal4-suppressor Gal80 to accurately regulate *serp* or *verm* expression. Using these flies, in histological experiments applying chitosan and chitin staining methods, Eosin Y in penetrations assays and atomic force microscopy (AFM) and transmission electron microscopy (TEM) in ultrastructural analyses, we demonstrate functional differences between *serp* and *verm* during *D. melanogaster* wing development.

2. Materials & methods

2.1. Drosophila strains and genetics

The hairpin RNA (hpRNA) coding uas-*serp*-RNAi (v15466) and uas-*verm*-RNAi (v15464) strains were from the Vienna *Drosophila* Resource Centre. The Gal4 driver lines nub-Gal4, tub-Gal80^{ts}, en-Gal4 and ap-Gal4 were a gift from Prof. Jie Shen at the China Agricultural University. w^{1118} was purchased from the Bloomington *Drosophila* Stock Centre. All *D. melanogaster* strains are raised at 25 °C with standard corn medium, while the cross lines of fruit fly are raised at 18 °C and shifted to 30 °C when the Gal4/UAS system is required to be derepressed.

For Gal80 inactivation experiments, adult flies were first allowed to lay eggs at 18 °C for 4 h. Next, the embryos were incubated at 18 °C for 24 h. For induction by temperature shift, animals were cultured in an incubator at 30 °C for 24, 48, 72, 108 or 120 h. Thereafter, they were placed back in an incubator with 18 °C until eclosion.

2.2. Image acquisition of the D. melanogaster wings and adults

Adults at day 3 after eclosion and their wings were selected for imaging using a Multifocus Imaging System of Fluorescence Microscope (MV PLAPO 1X, Olympus, Japan) equipped with a CCD camera (DFC450 C, Leica, Germany). For each experiment, we set three repeats and collected at least 35 offspring individuals per repeat. Average respective values of three repeats were calculated after calculating the average values of individuals in each tube.

2.3. Reverse transcription quantitative PCR (RT-qPCR)

The cDNA sequences of *serpentine*, *vermiform* and the reference gene *ribosomal protein 49* (*rp49*) were obtained from NCBI database. Specific RT-qPCR primers were designed using Primer Premier 5.0. The primer sequences are listed in Table 1. Total RNA from the wing discs of the 3rd instar larvae (30 wing discs for each repeat) or the pupal wing buds (100 buds for each repeat at the white pupal stage, 36 h post pupation at 30 °C) was extracted using Arcturus™ CapSure™ LCM MicroCaps (Thermo Fisher Scientific, USA) or RNAisoTM Plus (TaKaRa, Japan), respectively. Of note, RNA extraction of wing buds may have contamination of surrounding tissues. 1 μg of total RNA was used to synthesize the first-strand cDNA using M-MLV Reverse Transcriptase (Promega, USA) with an oligo-(dT) 18 primer (TaKaRa, Japan). The cDNA samples were diluted 40 times and used for RT-qPCR analysis. The reaction solution consisted of 10 μl of SYBR Green qPCR Master Mix (TOYOBO, Japan), 4.4 μl of deionized water, 4 μl of diluted template, and 0.8 μl of 0.4 μM forward and reverse primers, respectively. The qPCR conditions were as follows: denaturation at 95 °C for 1 min followed by 40 cycles at 95 °C for 15 s, 60 °C for 31 s on an ABI 7300 real time PCR machine (Applied Biosystems). A melting curve was determined for each sample to detect the gene-specific peak and checked for the absence of primer-dimers. We applied the $2^{-\Delta\Delta}C_T$ method to quantify gene expression. Three independent biological and two technical repetitions were performed. *t*-test was applied for biological statistics analysis.

Table 1
Primers for PCR amplification.

Gene	Primer	Primer Sequences	Product Size (bp)
rp49	Forward	GACAGTATCTGATGCCCAACA	170
	Reverse	CTTCTTGGAGGAGACGCCGT	
serp	Forward	CACTGGCGATGGTTTCTTCT	126
	Reverse	GCTAGGGCTTAGGGTTTGGT	
verm	Forward	GTGGCTGAAGTCGAAGAAGG	205
	Reverse	GTTGGGCAGAGAGCAGTAGG	
Gal4	Forward	CACAACCAATTGCCTCCTCT	220
	Reverse	GGGTTTGGTGGGGTATCTTC	

2.4. FB28 staining

Fluorescent brightener 28 (FB28), according to Sigma-Aldrich (Germany) a chitin-detection dye, along with chitin binds weakly to other polysaccharide such as glycogen and DNA (Moussian et al., 2005). Adult flies at day 3 after eclosion were selected for dissecting the wings, and then wings were cut along the antero-posterior (A-P) boundary for FB28 staining experiments. First, the wings were fixed in 4% paraformaldehyde phosphate buffer (PBT 375 μl, 4% paraformaldehyde 20 μl, 0.1% Trion-X100 3.9 μl) for 6–8 h, subsequently, using phosphate buffer they were rinsed for 8 h before staining with FB28 solution (1 mg/ml) for 24 h. After rinsing the specimens in PBT buffer for 3 h, they were on an inverted Fluorescence Microscope (EVOS FL, Elife, USA).

2.5. Eosin Y penetration assay

Day 3 adult flies were prepared for the Eosin Y penetration assay. Whole flies were incubated in the dye solution (Eosin Y 0.5% (W/V) (Sigma-Aldrich, America) which is a form of Eosin and most commonly used as an acidic red stain and 0.1% Triton X-100) at 55 °C for 35 min (Wang et al., 2016, 2017) in Thermostatic Metal incubators (Bori, Hangzhou, China). Flies were then washed with water and the wings were cut for imaging by Multifocus Imaging System of Fluorescence Microscope.

2.6. Chitosan staining

A specific chitosan staining method was described to detect chitosan based materials (Rossomacha et al., 2004), which showed chitin deacetylation through the chromogenic reaction between chitosan (a positively charged biomaterial) and Fast Green (an anionic dye). Chitosan with high deacetylation levels is easily detected by this method, whereas chitin or chitosan with low deacetylation levels are hardly detected. As shown in Supplementary Fig. 1, wild-type larvae are stained by Fast Green, while *serp*, *verm* double mutant larvae fail to be stained. Adult fly wings after 1 h of eclosion were dissected for staining. Besides staining the whole wings, we also cut the wings of the Gal80^{ts},

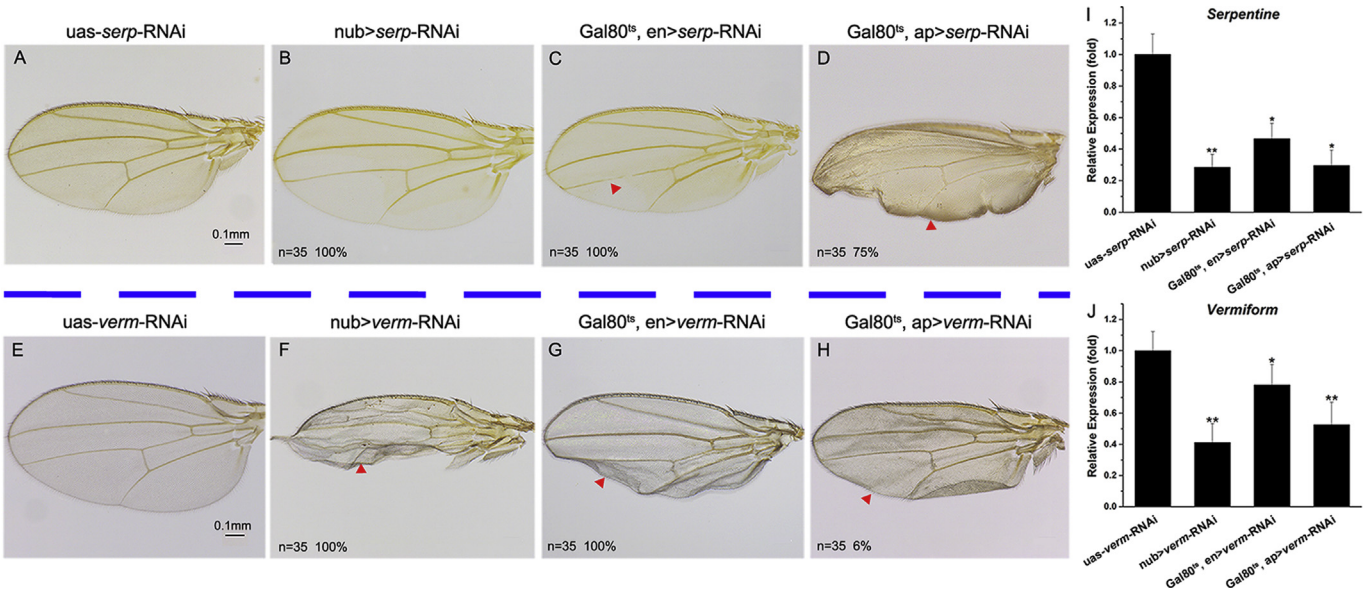

Fig. 1. Knockdown of *serp* or *verm* results in defects of *Drosophila* adult wings
(A, E) Wild-type wings of uas-*serp*-RNAi and uas-*verm*-RNAi flies are oval shaped. (B) The shape of nub > *serp*-RNAi wings was normal. (F) Wings from nub > *verm*-RNAi flies showed a crinkled phenotype. (C) The 4th wing vein of Gal80^{ts}, en > *serp*-RNAi wings was pale and thin. (G) In *verm*-knockdown flies, the posterior area of the wings appeared crinkled. (D) 75% of wings of Gal80^{ts}, ap > *serp*-RNAi flies showed a blistered phenotype. (H) 6% of wings of Gal80^{ts}, ap > *verm*-RNAi flies had a crinkled phenotype. (I, J) Expression of *serp* or *verm* in the pupal wing primordia (36 h after pupation at 30 °C) after RNAi using the three different Gal4 drivers. The red arrowheads point to wing defects compared with wild-type wings. Wing colour differences are due to different genetic backgrounds (Fig. S2). (For interpretation of the references to colour in this figure legend, the reader is referred to the Web version of this article.)

en > GFP, Gal80^{ts}, en > *serp*-RNAi and Gal80^{ts}, en > *verm*-RNAi fly lines along the antero-posterior (A-P) boundary. The staining method was slightly modified as follows: wings were fixed in 4% paraformaldehyde solution (PBT 375 μl, 4% paraformaldehyde 20 μl, 0.1% Trion-X100 1.95 μl) for 3 h. Wings were stained in 0.1% Fast Green (Sigma-Aldrich, USA) solution (0.1 g Fast Green in 1000 ml ddH_2O) for 48 h (Bright green). The chitosan signal of images of the wing cuticle was acquired by the image studio software (Licor, USA) by using a light microscope (Olympus, Japan).

2.7. Atomic force microscopy

The adult wing membrane was cut into small pieces and pasted onto a mica sheet (Yasheng Science, China) with a double-sided adhesive tape. The topography and force-displacement (F-Z) curves on the wing membrane surface were measured by contact mode using Atomic Force Microscope Multimode 8.0 from Bruker (USA). The piezoelectric scanner of the AFM is able to detect a maximum area about 10×10 μm^2 of the fly wing membrane. In these experiments, samples were kept at ambient air conditions with a relative humidity of 40% and a temperature of 23 °C. The typical commercial Si_3N_4 cantilevers used have a triangle tip and a force constant of approximately 0.4 N/m. The actual cantilever stiffness was measured by Thermal Yune's method. To further understand the wing membrane structure, a comparison of roughness data on wing membrane surface and mean height of the nanoscale bumps were analyzed by the Nanoscope Analysis 1.7 software. Roughness of the surface was calculated from the equation: $R_q = \sqrt{\frac{\sum (Z_j)^2}{N}}$ where Rq is the root mean square average height deviation taken from the mean image data plane, z is the height of surface point, and N is the numbers of measuring points. Mean height of the nanoscale bumps showed the absolute height of the bumps within a specified area.

2.8. Transmission electron microscope (TEM)

TEM was performed as described in (Li et al., 2017). Whole wings of day 3 Gal80^{ts}; nub > GFP, Gal80^{ts}; nub > *serp*-RNAi, and Gal80^{ts}; nub > *verm*-RNAi flies that were raised at 30 °C after eclosion were dissected, and fixed with 3% glutaraldehyde for 48 h at 4 °C. Thereafter, wings were rinsed 3–4 times with phosphate buffer followed by post-fixation in 1% osmium tetroxide for 3 h at 4 °C. The samples were put into the following concentration of acetone: 50, 70, 80, 90 and 100% for dehydration in 10 min. After washing twice, wings were embedded in Epon 812 at room temperature for 2 h. The samples were trimmed to prepare ultrathin sections. Ultrathin sections of wings from different fly lines were stained with 4% uranyl acetate and the ultrastructure of the wing cuticle was observed by a JEM-1200EX transmission electron microscope (TEM, JEOL, Japan).

3. Results

3.1. Serp and Verm are required for normal D. melanogaster wing development

In order to better understand the function of Serp and Verm during *D. melanogaster* wing development, we performed RNA interference (RNAi) experiments crossing uas-*serp*-RNAi or uas-*verm*-RNAi fly lines with three Gal4 driver lines that express Gal4 selectively in different regions of the wing imaginal discs (Fig. S2).

To knockdown *serp* and *verm* expression in the whole wing imaginal discs we used nub-Gal4. After depletion of *verm* (nub > *verm*-RNAi), wings showed a crinkled shape and an ectopic wing vein was present in one of the wing cells in contrast to the normal wings of uas-*serp*-RNAi, uas-*verm*-RNAi or nub > *serp*-RNAi flies (Figs. 1 and S3). Knockdown of *serp* or *verm* in the posterior half of the wing was induced using the en-Gal4 driver. Knockdown of *serp* in this region caused a very subtle phenotype. A portion of the fourth wing vein was missing compared with the control wing (Figs. 1C and S4E). To quantify this phenotype, we determined the ratio of the length of the "missing" region to the full length of the vein (Fig. S5). Knockdown of *verm* in this region resulted in 100% of curling of the posterior area of the wings (Figs. 1G and S4F). To suppress expression of *serp* or *verm* in the dorsal half of the wing, we

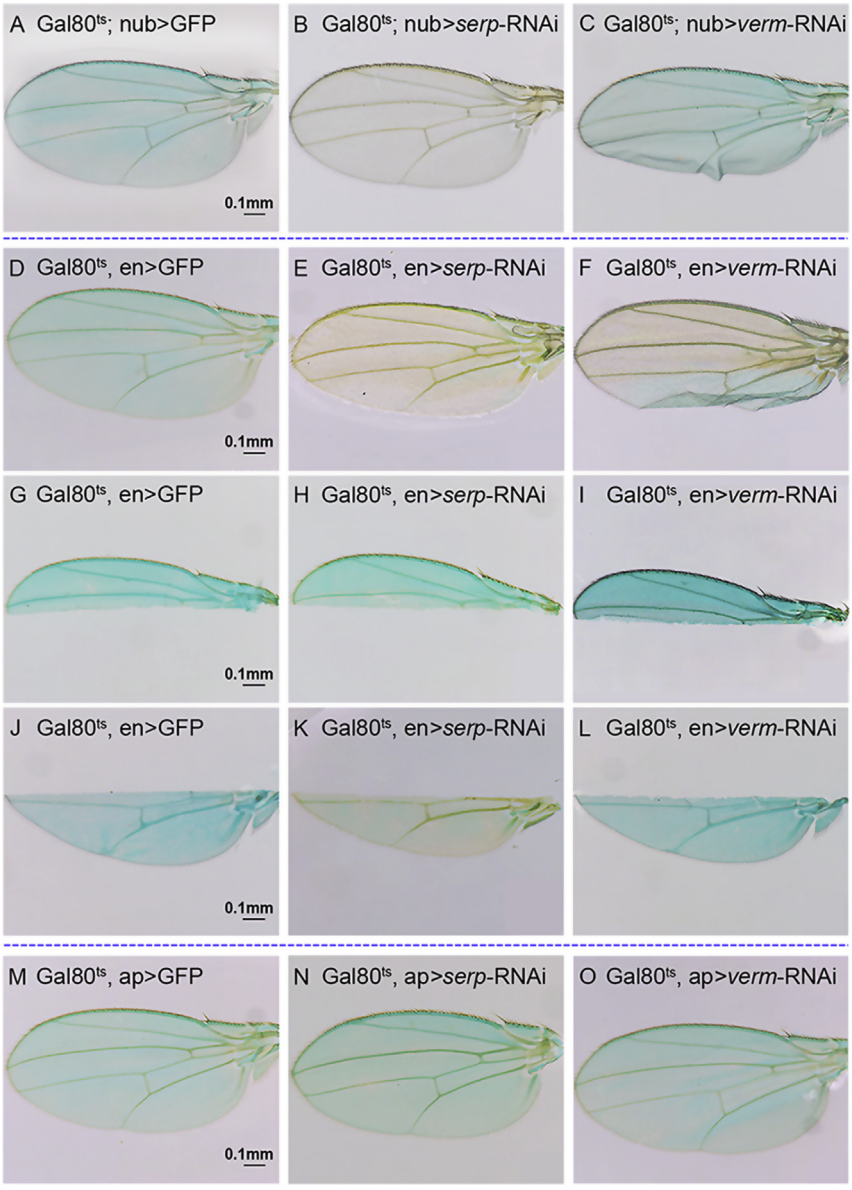

Fig. 2. Detection of chitosan after down regulating the expression of *serp* or *verm* in different areas of wings

(A, D, G, J, M) Control wings were light blue after staining with Fast Green. (B) Reduction of *serp* expression in the whole wing caused lack of Fast Green staining. (C) Reduction of *verm* expression had no effect on Fast Green staining. (E) Reduction of *serp* expression in the posterior half of the wing caused lack of Fast Green staining in the whole wing. (F) Reduction of *verm* expression in the posterior half of the wing provoked an unsteady staining. To enhance staining, we cut the wings with *serp* or *verm* suppression in the posterior half along the posterior-anterior axis. (H, K) The posterior half of wings with posterior *serp* suppression, remained unstained in this experiment, while the anterior half was positively marked. (G, J, I, L) Like control wings, wings with *verm* suppression at the posterior half, were fully stained. (N, O) Suppression of *serp* or *verm* in the dorsal half of the wing did not prevent full staining of the wing blade.

Of note, due to the long incubation time, Fast Green staining is variable. Detection of chitosan after Fast Green staining is therefore difficult to quantify between individual wings. Because of the thicker cuticle, wing veins appear darker within the same wing than wing membranes. Scale bar is 0.1 mm. (For interpretation of the references to colour in this figure legend, the reader is referred to the Web version of this article.)

used the ap-Gal4 driver. Wings of ap > *serp*-RNAi flies were blistered in 75% of cases (Figs. 1D and S4H). By contrast, only 6% of ap > *verm*-RNAi flies exhibited overt changes in wing shape (Figs. 1H and S4I). Interestingly, defects in notum formation were observed in these flies (Fig. S4I). These results suggest that Serp and Verm are essential for wing formation and that their functions differ during wing development.

To verify whether RNAi induced down-regulation of *serp* and *verm* expression was successful, we examined the expression profiles of their transcripts in the wing primordia of respective RNAi flies at 36 h (30 °C) after pupating (Fig. 1I and J). Wing primordia of uas-*serp*-RNAi and uas-*verm*-RNAi flies were used as controls. Of note, during wing primordia preparation, we were unable to avoid contamination from surrounding tissues. We found that *serp* and *verm* expression was partially down-regulated in the respective flies with a silencing efficiency higher than 65% compared with transcript levels in wild-type flies. We additionally determined the efficiency of *serp* and *verm* RNAi in 3rd instar larval wing discs during *serp* and *verm* hpRNA expression by the three different Gal4 drivers (Fig. S6). We found that *serp* and *verm* expression was down-regulated in the respective imaginal discs. Especially, nub > Gal4 driven hpRNA expression considerably suppressed *serp* or *verm* expression. As expected because of tissue portions without suppression, wing discs with ap > Gal4 and en > Gal4 had comparably higher *serp* and *verm* transcript levels after RNAi induction.

3.2. Knockdown of serp, not verm, disrupts chitin-chitosan conversion

To determine the deacetylation ability of Serp and Verm, we analyzed the deacetylation degree of *serp* or *verm*-depleted wings applying a Fast Green staining protocol (Rossomacha et al., 2004). The whole wing was stained by Fast Green in the three different Gal4 control fly lines as well as in the Gal80^{ts}; nub > *verm*-RNAi, (Gal80^{ts}, ap > *verm*-RNAi) and (Gal80^{ts}, ap > *serp*-RNAi) fly lines (Fig. 2A, C, D,M and O). The posterior wings of the Gal80^{ts}, en > *verm*-RNAi flies were also stained (Fig. 2F). By contrast, the wings of Gal80^{ts}; nub > *serp*-RNAi and Gal80^{ts}, en > *serp*-RNAi flies remained unstained after incubation with Fast Green (Fig. 2B and E).

Unexpectedly, both the anterior and posterior areas of Gal80^{ts}, en > *serp*-RNAi wings and the anterior half of Gal80^{ts}, en > *verm*-RNAi wings were unstained (Fig. 2E and F). We reckon that the genetic background of Gal80^{ts}, en > *serp*-RNAi or en > *verm*-RNAi blocked Fast Green penetration through the cuticle. In order to allow dye

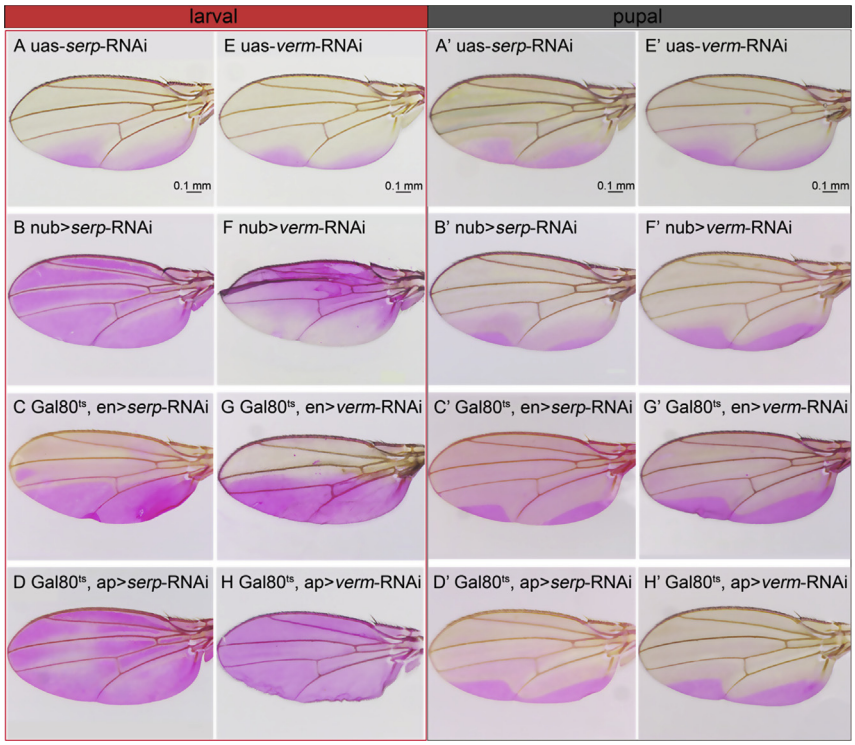

Fig. 3. The functional period of *serp* or *verm* during *Drosophila* wing development
(A, B) Eosin Y penetrates two areas in the posterior half of the control wing at 55 °C. Suppression of *serp* or *verm* caused excessive Eosin Y penetration in the area of suppression induced during larval stages (upper panels). Suppression of neither *serp* nor *verm* induced during pupal development changed the Eosin Y penetration pattern (lower panels).

penetration, we cut the wings along the anterior-posterior boundary before staining with Fast Green. The posterior area of the wings was faintly stained in Gal80^{ts}, en > *serp*-RNAi flies, while the anterior area of these wings was clearly stained (Fig. 2H and K). By contrast, both halves of Gal80^{ts}, en > *verm*-RNAi and Gal80^{ts}, en > *GFP* control wings were stained (Fig. 2G, J, 2I and 2L). Taken together, we carefully conclude that the function of Serp might be to convert chitin to chitosan whereas Verm does not seem to have any detectable deacetylation activity.

3.3. Serp and verm are needed for wing cuticle impermeability and wing vein stability

To investigate whether Serp and Verm function is required for wing cuticle impermeability, we incubated the wings of the RNAi flies in an Eosin Y solution (Wang et al., 2016). In control wings, two areas in the posterior half were stained by Eosin Y at 55 °C (Fig. 3A, 3A′, 3E and 3E'). Suppression of *serp* or *verm* expression in the entire wing of Gal80^{ts}; nub > *serp*-RNAi or Gal80^{ts}; nub > *verm*-RNAi flies at the larval stage caused penetration of Eosin Y in the whole wing (Fig. 3B and F). Likewise, the whole wing of Gal80^{ts}, ap > *serp*-RNAi or Gal80^{ts}, ap > *verm*-RNAi flies with reduced *serp* or *verm* expression in the dorsal half of the tissue induced at the larval stage, respectively, were stained by Eosin Y (Fig. 3D and H). Finally, Eosin Y penetrated the posterior half of the wings of Gal80^{ts}, en > *serp*-RNAi or Gal80^{ts}, en > *verm*-RNAi flies which were driven at larval stages (Fig. 3C and G). These results together indicate that reduced expression of Serp and Verm enhance local wing cuticle permeability.

To characterize the influence of Serp and Verm on wing vein cuticle, we investigated the penetration of FB28, a polysaccharide-specific dye, into the cut wing vein cuticle (Fig. S7). In control Gal80^{ts}; nub > *serp*-RNAi, Gal80^{ts}; nub > *verm*-RNAi and Gal80^{ts}, ap > *verm*-RNAi fly wing veins, penetration of FB28 is restricted to the veins (a-b' in Fig. S7A and S7B, d and d' in Fig. S7B), whereas in (Gal80^{ts}, en > *serp*-RNAi), (Gal80^{ts}, en > *verm*-RNAi) and (Gal80^{ts}, ap > *serp*-RNAi) flies FB28 flowing through the veins laterlly diffused to some extent into the blade cuticle (c' in Fig. S7A and S7B, d and d' in Fig. S7A). In summary, Serp and Verm are needed for wing vein cuticle integrity.

3.4. Larval expression of serp and verm is essential for wing cuticle formation

To determine the precise period of *serp* or *verm* gene requirement, we sought to induce Gal4 activity at different time points during fly development using the temperature-sensitive Gal4 suppressor Gal80^{ts} in combination with nub-Gal4, en-Gal4 and ap-Gal4 in RNAi experiments. To monitor *serp* or *verm* activity, we observed the areas of Eosin Y penetration after knockdown of *serp* or *verm* in Eosin Y penetration assays during (Figs. 3 and S8). Deactivation of Gal80^{ts} during pupal stages of nub > *serp/verm*-RNAi, en > *serp/verm*-RNAi or ap > *serp/verm*-RNAi flies did not have any effect on Eosin Y penetration into wings. This unexpected result may be due to low RNAi efficiency during pupal stages when Gal4 expression declines (Fig. S2). Deactivation of Gal80^{ts} during larval stages did not induce Eosin Y penetration into wings of *serp*-RNAi expressing flies until 108 h post-hatching (third instar larvae). Ectopic penetration of Eosin Y into these wings occurred when Gal80^{ts} was deactivated 120 h post-hatching. Eosin Y penetration into the wings of *verm*-RNAi was observed when Gal80^{ts} was deactivated 96 h post-hatching or later (Fig. S8). These data suggest that Serp and Verm are needed for the construction of the wing barrier at different time points.

3.5. Suppression of serp or verm affects the structure of the wing surface

The wing membrane is decorated with bristles and nanoscale bumps (Li et al., 2017; Wagner et al., 2012). Changes in the wing cuticle matrix may result in changes in the shape of surface structures. To test this hypothesis, the wing membranes of nub > *serp/verm*-RNAi, en > *serp/verm*-RNAi or ap > *serp/verm*-RNAi lines were imaged with an atomic force microscope (AFM). There were regularly spaced nanoscale bumps on the wing surfaces of the different control fly lines (Fig. 4A). On the wings of Gal80^{ts}; nub > *serp*-RNAi flies, the nanoscale bumps were quasi absent (Fig. 4B), while on Gal80^{ts}; nub > *verm*-RNAi wings, they appeared to be thicker than those on the control wings and

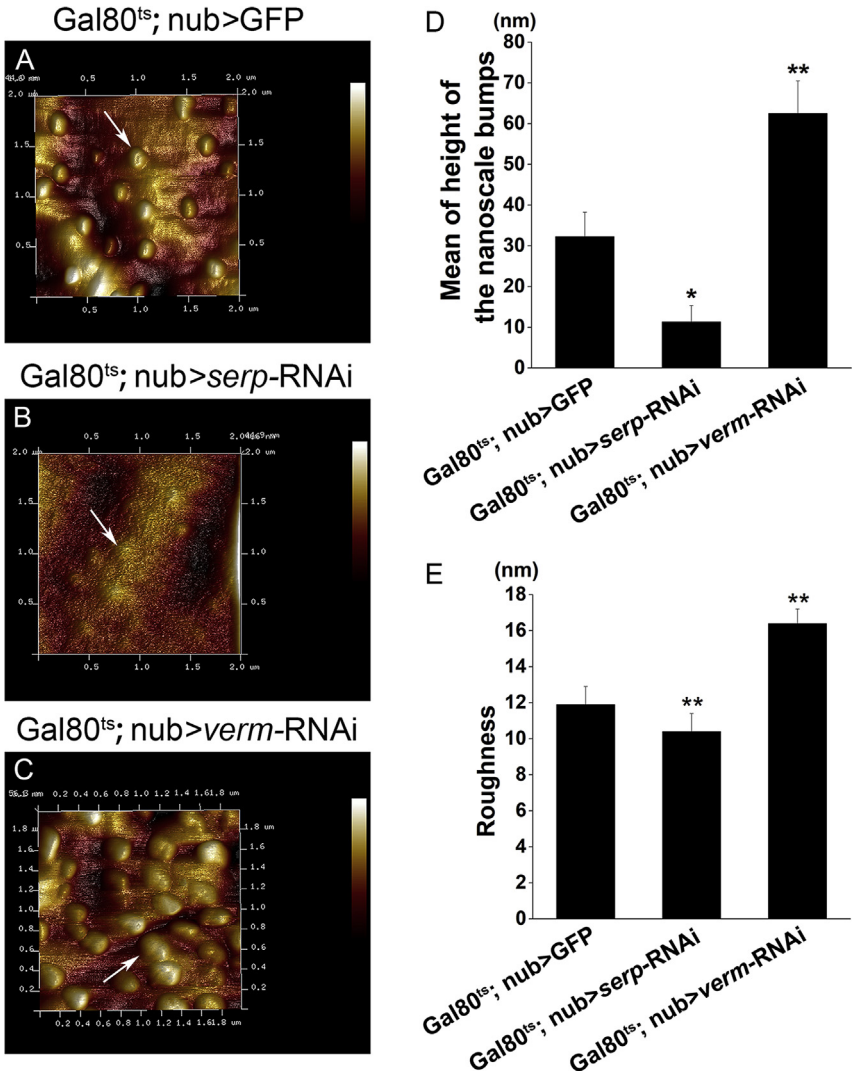

Fig. 4. Long range atomic force microscope (AFM) topography scans of wing membrane surfaces of control, *serp* or *verm* down-regulating flies
(A-C) Regularly spaced bumps cover the surfaces of control and *serp* or *verm*-reduced wings. (arrow, A, D) These bumps are dome-shaped (arrow) with a height of around 30 nm in control flies. (B, D) They are shorter (arrow, around 10 nm) or thinner after *serp* suppression. (C, D) They are taller (arrow, around 60 nm) or thicker when *verm* is down regulated. Compared to control, surface roughness is also significantly changed when *serp* or *verm* expression is suppressed (E).

occasionally split into two parts (Fig. 4C). Using these images, we measured the mean height of the nanoscale bumps in dependence of Verm or Serp function (Fig. 4D). Nanoscale bumps were dramatically reduced in size (0.31 fold) on Gal80^{ts}; nub > *serp*-RNAi wings. By contrast, nanoscale bump size was increased (1.94 fold) on Gal80^{ts}; nub > *verm*-RNAi wings. Consistently, roughness of the wing surface is significantly raised in Gal80^{ts}; nub > *verm*-RNAi flies, but is significantly reduced in Gal80^{ts}; nub > *serp*-RNAi flies (Fig. 4E). Thus, Serp and Verm have distinct effects on wing surface structure.

3.6. *Verm but not Serp is needed for laminar organisation of the wing procuticle*

We next analyzed the effects of *verm* and *serp* down-regulation on the wing cuticle ultrastructure (Fig. 5 and Fig. S9). The wing cuticle of Gal80^{ts}; nub > *GFP* control flies consists of a thick laminar procuticle and a thin epicuticle. In Gal80^{ts}; nub > *serp*-RNAi flies, the wing cuticle matrix structure was normal. By contrast, in Gal80^{ts}; nub > *verm*-RNAi flies, the laminar organisation of the procuticle was lost. In summary, Verm is required for the laminar organisation of the wing cuticle while Serp is not.

4. Discussion

In a series of articles, the laboratory of Matthias Behr reported that in the assembly zone of the *D. melanogaster* cuticle, where chitin fibres are deposited and organised adjacent to the apical plasma membrane, the chitin deacetylases Serp and Verm, the chitin organising factors Knickkopf (Knk) and Obst-A and Chitinase2 interact during cuticle formation in *D. melanogaster* larvae (Pesch et al., 2017). As shown here and previously (Li et al., 2017), Knk, Serp and Verm are also active during wing cuticle formation. As we know that at least Chitinase2 is also present in this tissue (Sobala and Adler, 2016), we conclude that the chitin organisation machinery is conserved in larvae and the wing. Interestingly, at least *knk* and *serp/verm* expression is under the control of different signalling pathway suggesting a more complex situation at the transcriptional level (Gangishetti et al., 2012). Our data presented here indicate moreover that the two chitin deacetlyases Serp and Verm have non-redundant functions during cuticle formation, but common roles in cuticle barrier function.

4.1. *Serp is the major chitin deacetylase in the fly wing*

CDAs, which belong to the family of carbohydrate esterases (CE 4),

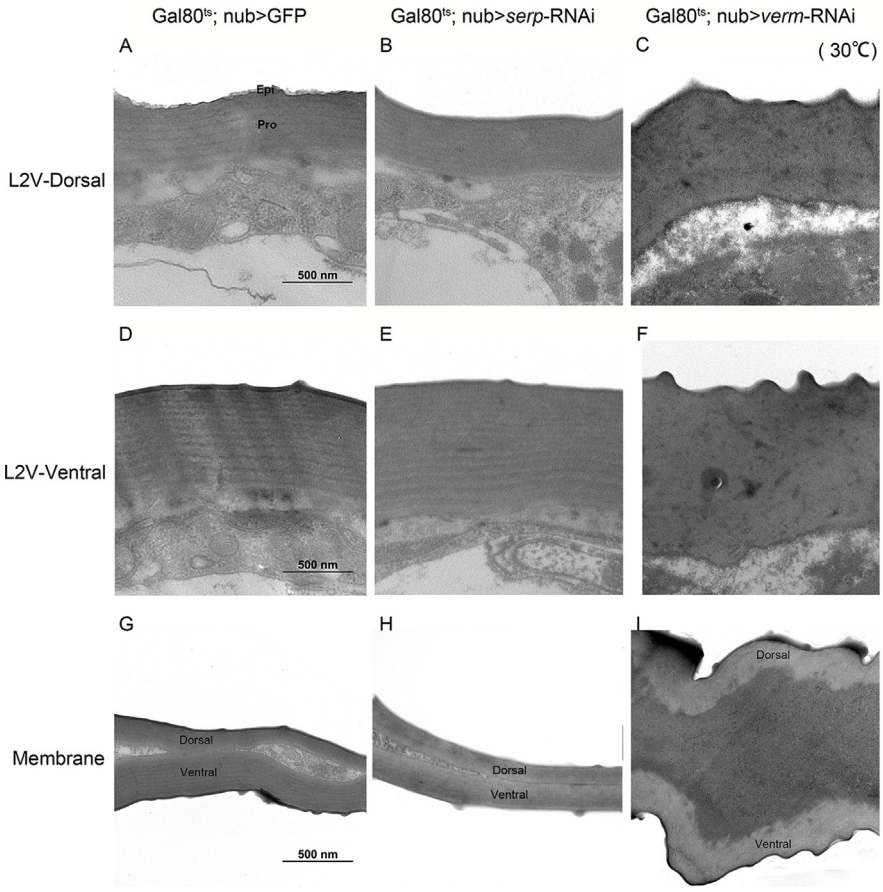

Fig. 5. Ultrastructure of the wing cuticle in control and *serp* or *verm* suppressed flies

The ventral and dorsal cuticles of control and *serp* suppressed wings at the position of the L2 vein and in the wing membrane consists of a laminate procuticle and the above epicuticule (A, B, D, E, G, H). The procuticle of the ventral and dorsal cuticle of *verm* knock-down wings at the same positions is not laminate (C, F, I). Additionally, it has lost its compactness. The irregularities at the surface of this cuticle may stem from the nanoscale bumps. In the membrane of control wings and of wings with reduced *serp* expression, the dorsal and ventral cuticles are laminar and contact each other (G, H). In the membrane of wings with reduced *verm* expression, the dorsal and ventral cuticles detach from each other (I).

The outermost envelope is not visible in these electron-micrographs. L2V: longitudinal 2 vein, Epi: Epicuticle; Pro: Procuticle.

modify chitin to chitosan. Neville (1975) speculated on the importance of this reaction in defining the physical properties of the cuticle. Among others, he proposed that different proteins may bind to either polysaccharide. Although it was repeatedly shown that the group I CDAs CDA1 and CDA2 are both essential for normal insect development (Arakane et al., 2009; Campbell et al., 2008; Luschnig et al., 2006; Quan et al., 2013; Wang et al., 2006), the enzyme indeed responsible for chitin deacetylation had not been identified. Using a chitosan staining assay, we demonstrate that Serp is the major chitin deacetylase, while Verm has no detectable effect on chitosan levels in the wing cuticle. This finding is in line with a recent report on the function of CDA1, the orthologue of Serp and CDA2, the orthologue of Verm in the nymphal cuticle of the migratory locust *Locusta migratoria* (Yu et al., 2018). Moreover, the Verm CDA domain lacks important amino acids arguing that it is not a functional CDA (Luschnig et al., 2006). Thus, we propose that in insects in general CDA1 is the major chitin deacetylase in the cuticle.

4.2. Procuticle laminar organisation is independent of Serp but requires Verm

According to a theory formulated by Neville (1975), chitosan and chitin are recognised and bound by different proteins thereby defining the physical properties of the cuticle. A central question is as to what extent the chitin-chitosan ratio accounts for procuticle laminar structure. We show that down-regulation of Serp (CDA1) and by consequence lack of bulk chitosan does not interfere with the laminar organisation of the procuticle. Down-regulation of Verm (CDA2), by contrast, that does not cause detectable reduction of chitosan, has a dramatic effect on procuticle laminar structure and the chitin matrix loses its compactness. The situation is identical in *L. migratoria*, a hemimetabolous insect (order Orthoptera), which is only distantly related to *D. melanogaster* (order Diptera): CDA2 like Verm is needed for the laminar organisation and compactness of the procuticle in nymphs (Yu et al., 2016), while CDA1 like Serp is dispensable for this process (Yu et al., 2018). The situation is different in *T. castaneum*, a holometabolous insect (order Coleoptera), which is, compared to *L. migratoria*, closely related to *D. melanogaster*. Noh et al. observed a severe loss of laminar organisation in the cuticle of the soft hindwing and the rigid elytron after RNAi against *TcCDA1* or *TcCDA2* (Noh et al., 2018). They found that short chitin fibrils are enriched upon depletion of *TcCDA1* and *TcCDA2*. Of course, the chitin deacetylation capacity of TcCDA1 and TcCDA2 remains to be tested. In summary, they proposed that elongation of chitin nanofibers and their as well arrangement at the higher order structures depends on deacetylation. This is apparently not the case in *D. melanogaster* wings and in *L. migratoria* nymphs. Taken all these findings and observations together, we hypothesize that CDA1 and CDA2 activities vary in insect orders irrespective of the evolutionary relationship.

4.3. Cuticle barrier function depends on Serp and Verm

Wang et al. found that the insect cuticle inward barrier involves surface lipids and is temperature-dependent using an Eosin Y penetration assay (Wang et al., 2016, 2017). Here, we found that knockdown of *serp* or *verm* transcripts increased the penetration area of Eosin Y on the adult fly wings. Surprisingly, this knockdown induced during larval stages was sufficient to interfere with the cuticle barrier function. Possibly, transcript accumulation or protein storage in the cells of wing imaginal discs during larval development is a crucial process for Serp and Verm function. In any case, we conclude that an – not necessarily morphologically - intact procuticle is essential for the inward barrier function of the cuticle. Our previous finding that Knickkopf (Knk), a chitin-organising protein is required to prevent xenobiotic penetration

into the wing cuticle supports this conclusion (Li et al., 2017). The ultrastructural differences between *serp* and *verm* depleted wings allows moreover concluding that the laminar organisation of the procuticle is not per se contributing to the barrier function.

4.4. Serp and Verm change the surface of Drosophila wing membrane

Nanostructures on the wing surface of insects have been reported to be involved in self-cleaning, hydrophobicity, and aerodynamic drag reduction of the wing (Byun et al., 2009; Watson et al., 2008, 2010). In *D. melanogaster*, different types of wing surface structures have been described (Wagner et al., 2012). 100 nm bumps corresponding to the nanoscale bumps presented in this work, are proposed to contribute to surface hydrophobicity. Penetration problems in *serp* and *verm* depleted wings, hence, may be due to changes in the wing surface structure. In *serp*-less wings, the nanoscale bumps are almost missing probably causing loss of penetration protection. In *verm*-less wing, by contrast, the nanoscale bumps are misshapen and bigger than on control wings. This defect may reduce optimal protection against penetration. Consistently, the nanoscale bumps on wings with down-regulated *knk* expression are comparably small and xenobiotic penetration into these wings is enhanced (Li et al., 2017). Together, these findings suggest that the procuticle may contribute to the inward barrier function of the cuticle by ensuring correct structuring of the wing surface.

Acknowledgments

This work was supported by the National Natural Science Foundation of China (Grant No. 31672364 and 31402021), the Program for Top Young Academic Leaders of Higher Learning Institutions of Shanxi (TYAL) 2017, the Natural Science Foundation of Shanxi Province, China, Grant 2015011070, 2018 Special Talents Project in Shanxi Province, China (Grant 201805D211019) and Shanxi Scholarship Council of China (Grant 2015-007). We thank Atomic Force Microscope Multimode 8.0 at Scientific Instrument Centre, Shanxi University, China. BM was supported by the German Research Foundation (DFG, Grants MO1714).

Appendix A. Supplementary data

Supplementary data to this article can be found online at https://doi.org/10.1016/j.ibmb.2019.05.008.

References

Arakane, Y., Dixit, R., Begum, K., Park, Y., Specht, C.A., Merzendorfer, H., Kramer, K.J., Muthukrishnan, S., Beeman, R.W., 2009. Analysis of functions of the chitin deacetylase gene family in Tribolium castaneum. Insect Biochem. Mol. Biol. 39, 355–365.

Byun, D., Hong, J., Saputra, Ko, J.H., Lee, Y.J., Park, H.C., Byun, B.-K., Lukes, J.R., 2009. Wetting characteristics of insect wing surfaces. J. Bionics Eng. 6, 63–70.

Campbell, P.M., Cao, A.T., Hines, E.R., East, P.D., Gordon, K.H., 2008. Proteomic analysis of the peritrophic matrix from the gut of the caterpillar, Helicoverpa armigera. Insect Biochem. Mol. Biol. 38, 950–958.

Dixit, R., Arakane, Y., Specht, C.A., Richard, C., Kramer, K.J., Beeman, R.W., Muthukrishnan, S., 2008. Domain organization and phylogenetic analysis of proteins from the chitin deacetylase gene family of Tribolium castaneum and three other species of insects. Insect Biochem. Mol. Biol. 38, 440–451.

Dong, B., Miao, G., Hayashi, S., 2014. A fat body-derived apical extracellular matrix enzyme is transported to the tracheal lumen and is required for tube morphogenesis in Drosophila. Development 141, 4104–4109.

Gangishetti, U., Veerkamp, J., Bezdan, D., Schwarz, H., Lohmann, I., Moussian, B., 2012. The transcription factor Grainy head and the steroid hormone ecdysone cooperate during differentiation of the skin of Drosophila melanogaster. Insect Mol. Biol. 21, 283–295.

Heustis, R.J., Ng, H.K., Brand, K.J., Rogers, M.C., Le, L.T., Specht, C.A., Fuhrman, J.A., 2012. Pharyngeal polysaccharide deacetylases affect development in the nematode C. elegans and deacetylate chitin in vitro. PLoS One 7, e40426.

Li, K., Zhang, X., Zuo, Y., Liu, W., Zhang, J., Moussian, B., 2017. Timed Knickkopf function is essential for wing cuticle formation in Drosophila melanogaster. Insect Biochem. Mol. Biol. 89, 1–10.

Luschnig, S., Batz, T., Armbruster, K., Krasnow, M.A., 2006. Serpentine and vermiform encode matrix proteins with chitin binding and deacetylation domains that limit tracheal tube length in Drosophila. Curr. Biol. 16, 186–194.

Moussian, B., 2010. Recent advances in understanding mechanisms of insect cuticle differentiation. Insect Biochem. Mol. Biol. 40, 363–375.

Moussian, B., Schwarz, H., Bartoszewski, S., Nusslein-Volhard, C., 2005. Involvement of chitin in exoskeleton morphogenesis in Drosophila melanogaster. J. Morphol. 264, 117–130.

Neville, A.C., 1975. Biology of the Arthropod Cuticle. Springer Verlag.

Noh, M.Y., Muthukrishnan, S., Kramer, K.J., Arakane, Y., 2018. Group I chitin deacetylases are essential for higher order organization of chitin fibers in beetle cuticle. J. Biol. Chem. 293, 6985–6995.

Pesch, Y.Y., Riedel, D., Behr, M., 2017. Drosophila Chitinase 2 is expressed in chitin producing organs for cuticle formation. Arthropod Struct. Dev. 46, 4–12.

Quan, G., Ladd, T., Duan, J., Wen, F., Doucet, D., Cusson, M., Krell, P.J., 2013. Characterization of a spruce budworm chitin deacetylase gene: stage- and tissue-specific expression, and inhibition using RNA interference. Insect Biochem. Mol. Biol. 43, 683–691.

Rossomacha, E., Hoemann, C., Shive, M., 2004. Simple Methods for Staining Chitosan in Biotechnological Applications.

Sobala, L.F., Adler, P.N., 2016. The gene expression Program for the formation of wing cuticle in Drosophila. PLoS Genet. 12, e1006100.

Tsigos, I., Martinou, A., Kafetzopoulos, D., Bouriotis, V., 2000. Chitin deacetylases: new, versatile tools in biotechnology. Trends Biotechnol. 18, 305–312.

Vincent, J.F., Wegst, U.G., 2004. Design and mechanical properties of insect cuticle. Arthropod Struct. Dev. 33, 187–199.

Vollmer, W., Tomasz, A., 2000. The pgdA gene encodes for a peptidoglycan N-acetylglucosamine deacetylase in Streptococcus pneumoniae. J. Biol. Chem. 275, 20496–20501.

Wagner, R., Pittendrigh, B.R., Raman, A., 2012. Local elasticity and adhesion of nanostructures on Drosophila melanogaster wing membrane studied using atomic force microscopy. Appl. Surf. Sci. 259, 225–230.

Wang, S., Jayaram, S.A., Hemphala, J., Senti, K.A., Tsarouhas, V., Jin, H., Samakovlis, C., 2006. Septate-junction-dependent luminal deposition of chitin deacetylases restricts tube elongation in the Drosophila trachea. Curr. Biol. 16, 180–185.

Wang, Y., Carballo, R.G., Moussian, B., 2017. Double cuticle barrier in two global pests, the whitefly Trialeurodes vaporariorum and the bedbug Cimex lectularius. J. Exp. Biol. 220, 1396–1399.

Wang, Y., Yu, Z., Zhang, J., Moussian, B., 2016. Regionalization of surface lipids in insects. Proc. Biol. Sci. 283.

Watson, G.S., Cribb, B.W., Watson, J.A., 2010. The role of micro/nano channel structuring in repelling water on cuticle arrays of the lacewing. J. Struct. Biol. 171, 44–51.

Watson, G.S., Myhra, S., Cribb, B.W., Watson, J.A., 2008. Putative functions and functional efficiency of ordered cuticular nanoarrays on insect wings. Biophys. J. 94, 3352–3360.

Xi, Y., Pan, P.L., Ye, Y.X., Yu, B., Zhang, C.X., 2014. Chitin deacetylase family genes in the brown planthopper, Nilaparvata lugens (Hemiptera: Delphacidae). Insect Mol. Biol. 23, 695–705.

Yu, R., Liu, W., Li, D., Zhao, X., Ding, G., Zhang, M., Ma, E., Zhu, K., Li, S., Moussian, B., Zhang, J., 2016. Helicoidal organization of chitin in the cuticle of the migratory locust requires the function of the chitin Deacetylase2 enzyme (LmCDA2). J. Biol. Chem. 291, 24352–24363.

Yu, R.R., Liu, W.M., Zhao, X.M., Zhang, M., Li, D.Q., Zuber, R., Ma, E.B., Zhu, K.Y., Moussian, B., Zhang, J.Z., 2018. LmCDA1 organizes the cuticle by chitin deacetylation in Locusta migratoria. Insect Mol. Biol. https://doi.org/10.1111/imb.12554.